

*Research Article*

# Standardization of the elevation in the AW3D30 global digital elevation model to the Vietnamese national vertical datum: An experiment in Ninh Binh province and surrounding areas

Bui Thi Hong Tham<sup>1\*</sup>, Trinh Thi Hoai Thu<sup>1</sup>, Do Thi Hoai<sup>2</sup>

<sup>1</sup> Hanoi University of Natural Resources and Environment; bththam@hunre.edu.vn; tththu@hunre.edu.vn

<sup>2</sup> Vietnam Institute of Surveying and Mapping; hoaiVo1976@gmail.com

\*Corresponding author: bththam@hunre.edu.vn; Tel.: +84–976785816

Received: 17 January 2025; Accepted: 26 February 2025; Published: 8 June 2025

**Abstract:** This study proposes a method for normalizing the elevation of the global digital elevation model (GDEM) ALOS World 3D - 30 m (AW3D30) to Vietnam's national height system, based on national GNSS/levelling data from Ninh Binh province and surrounding areas. The correction process consists of three main steps: (1) Collecting GNSS/levelling data, global DEM data, and EGM96 geoid model data to ensure accuracy and consistency; (2) Determining correction parameters to transform AW3D30 global elevations to local heights, including analyzing differences between global and local geoid models and assessing tidal influences; (3) Verifying, correcting, and evaluating the accuracy of AW3D30 after correction to align with the national height system. Experimental results show that after correction, the root mean square error of the AW3D30 model in the national vertical datum is  $\pm 1.613$  m, while the maximum deviation between AW3D30 elevations and GNSS/levelling heights is reduced from 9.014 m to 5.238 m. Approximately 91.7% of GNSS/levelling points have deviations within the acceptable range, demonstrating that the correction method significantly enhances the accuracy and applicability of AW3D30 in the national vertical datum. This method not only facilitates the normalization of AW3D30 in the study area but can also be applied to other regions in Vietnam, as well as to other GDEMs. The research findings contribute to improving the accuracy of topographic data, supporting spatial planning, resource management, disaster forecasting, and related applications.

**Keywords:** AW3D30; National Vertical Datum; DEM; GNSS/levelling; Ninh Binh.

## 1. Introduction

The global digital elevation model (GDEM) is a crucial product of Earth sciences, serving as a foundational tool for various research fields and practical applications. The digital elevation model (DEM) provides topographic data at different levels of resolution, enabling a more detailed representation of the Earth's surface than traditional methods. As a result, DEM plays a key role in geological, geomorphological, hydrological, glaciological studies, and natural disaster risk assessments [1]. Due to its ability to depict large-scale terrain structures, DEM is not only an essential tool for terrain visualization and analysis [2–3] but also supports the simulation of natural processes [4–6] and provides critical information for infrastructure planning, climate change studies, disaster monitoring, and natural resource management [7–12]. Recent studies have demonstrated that DEM is essential for surface flow modeling, flood assessment, and identifying landslide-prone areas [13, 14]. Currently, several widely used global DEMs exist, including the shuttle radar topography mission

(SRTM), advanced spaceborne thermal emission and reflection radiometer global digital elevation model (ASTER GDEM), NASADEM, and AW3D30, which are extensively utilized in research and practical applications [15–17]. These GDEMs provide large-scale topographic data with relatively high resolution, contributing to improved accuracy in terrain, hydrology, and environmental change studies. Among them, AW3D30, developed by the Japan Aerospace Exploration Agency (JAXA) using ALOS satellite imagery, is considered one of the most accurate models [18, 19]. With a spatial resolution of 30 m, AW3D30 utilizes stereoscopic data collected by the ALOS PRISM satellite and applies advanced image processing algorithms to generate a high-quality terrain model. Studies have shown that the accuracy of AW3D30 is higher than that of other global DEM models such as SRTM and ASTER GDEM [20–23]. Therefore, AW3D30 is selected for this study to assess the model's suitability under experimental conditions.

Although the global digital elevation model AW3D30 provides topographic data over a wide area, a significant limitation is the discrepancy between the model's vertical reference system and the national height system. Specifically, AW3D30 uses the global geoid EGM96 (tide-free system), whereas Vietnam's official height system (HN-72) is based on the long-term mean sea level at the Hon Dau tide gauge in Hai Phong (tide-mean system).

This discrepancy leads to significant differences between the DEM-derived elevations and actual surveyed heights, as EGM96 does not accurately reflect the regional gravity field of Vietnam and is not consistent with the local height system, which is influenced by oceanographic and regional topographic factors. Moreover, the Hon Dau reference point is determined from long-term sea level observations, while EGM96 is a global model built on satellite gravity and geodetic data. This results in systematic errors that can reach several meters in certain areas. Study [20] also emphasizes that to minimize errors when applying DEMs to local studies, they must be standardized according to the national height system.

Standardizing the global DEM AW3D30 to the local height system not only improves accuracy but also ensures consistency in practical applications. However, this process is not a simple conversion but requires a combination of field measurements, error modeling, and accuracy assessment. One of the biggest challenges is the complexity of terrain, as differences in elevation modeling methods can introduce significant interpolation errors. Mountainous areas with steep elevation changes tend to have greater errors than plains or coastal regions due to abrupt height variations and uneven point density, which can reduce the accuracy of DEM correction. Additionally, tidal effects play an important role in height standardization, especially in coastal and estuarine regions. Sea level fluctuations caused by tidal cycles and oceanographic dynamic factors, such as currents and atmospheric pressure changes, can impact the determination of the reference height system, leading to discrepancies in DEM conversion. Finally, the difference between the global geoid model and the local geoid is a crucial factor that must be carefully considered, as the global geoid EGM96 does not accurately represent Vietnam's regional gravity field, resulting in nonlinear errors in height transformation. This necessitates appropriate geoid correction models to align the DEM's vertical coordinate system with the national height system. Therefore, to optimize the performance of DEMs in geographic and environmental science applications, a suitable correction approach must be applied, integrating local geoid correction models, actual elevation survey data, and accurate interpolation algorithms. This not only minimizes errors but also ensures that DEMs can be effectively used in terrain analysis, hydrology, and climate change studies.

Previous studies have proposed various DEM height correction methods to minimize discrepancies between global DEMs and national vertical reference systems [24]. Some common approaches include:

Ground control point (GCP)-based correction method: Utilizing known elevation points within the local vertical system to adjust the DEM. The elevation values of these points are

compared with the corresponding DEM elevations, and mathematical transformations are applied to correct the model [25–29].

Geoid model-based correction method: Employing geoid models to convert elevations from the global vertical system to the local datum [30–32].

Regression model-based correction method: Applying regression models to predict and remove systematic DEM errors based on terrain and climate factors [33–36].

LIDAR data-based correction method: Utilizing high-accuracy LIDAR data to refine GDEMs [37–39].

Artificial neural network (ANN)-based correction method: Using ANN models to learn and predict DEM errors, then applying trained algorithms to adjust the data [40, 41].

Kriging interpolation-based correction method: Applying kriging interpolation to detect and eliminate systematic DEM errors [42–46].

Additionally, combining multiple correction methods has been used in studies [40, 41], [45] to optimize accuracy.

Although elevation correction methods for DEMs improve accuracy when converting between global DEMs and national height systems, each method has its own limitations. Ground control point-based corrections depend on the distribution of survey points, while geoid model-based methods may introduce errors due to the limited accuracy of global geoid models. Regression models and artificial neural networks require high-quality training data, whereas Kriging interpolation is only effective when the data points are densely distributed. LIDAR data offers high accuracy but is expensive to collect and has limited coverage. Combining multiple methods can optimize correction efficiency, but it also increases computational complexity and challenges in result evaluation. Therefore, selecting an appropriate correction method requires careful consideration of factors such as terrain conditions, available data, and accuracy requirements for specific applications.

In this context, studies in Vietnam have focused on assessing and improving the accuracy of DEMs, particularly the SRTM model, to align with the national height system. These studies have compared SRTM-derived elevations with actual survey data from GNSS/levelling points [47–49] or with elevation data extracted from topographic maps [47, 50]. Additionally, some studies have proposed correction methods to reduce DEM errors for practical applications [48–49].

The results of the aforementioned studies indicate that while SRTM can be applied in Vietnam, it requires standardization to ensure higher accuracy, particularly in areas with complex terrain. Among the methods studied, using GNSS/levelling data is an optimal solution because these points have elevations directly determined in the national height system, eliminating errors caused by differences between height systems. Compared to topographic map data, GNSS/levelling provides higher accuracy and more accurately reflects terrain conditions at the time of measurement, avoiding compounded errors from interpolation or digitization processes. This method not only allows for a direct assessment of DEM deviations relative to the local height system but also provides a reliable dataset for systematically correcting DEMs, forming a foundation for further research and practical applications.

Therefore, this study focuses on using GNSS/levelling data to correct the global digital elevation model AW3D30 according to Vietnam's national height system. Specifically, high-precision and reliable first-order, second-order, and third-order GNSS/levelling data from national networks will be utilized. These points are measured simultaneously using GNSS and levelling techniques, providing both ellipsoidal and orthometric heights, thereby enabling a robust and reliable correlation between the global height system, global geoid models, and Vietnam's national height system.

The primary distinction of this study from previous research [47, 48, 50] is that GNSS/levelling data is not only used for comparing elevations between global models and

actual survey data but also plays a crucial role in the correction process. Influencing factors include tidal effects, discrepancies between global and local geoid models, and the accuracy of AW3D30 when converted to the national height system. While this issue was addressed in [49] for the SRTM model, AW3D30 has the potential to provide more precise terrain data and warrants further investigation [51–53].

To ensure a systematic correction process, this study proposes a three main steps: (1) Collecting GNSS/levelling data, global DEM data, and EGM96 geoid model data to ensure accuracy and consistency; (2) Determining correction parameters to transform AW3D30 global elevations to local heights, including analyzing differences between global and local geoid models and assessing tidal influences; (3) Verifying, correcting, and evaluating the accuracy of AW3D30 after correction to align with the national height system.

The experimental area selected for this study is Ninh Bình province and its surrounding regions, which feature diverse topography, including low-lying plains, dense river networks, and low mountainous areas. The selection of this area aims to concretize the proposed correction method while assessing the accuracy of the AW3D30 global DEM. The results obtained will serve as a critical foundation for evaluating the feasibility of applying this model in practical scenarios. The proposed correction method in this study can be extended to other regions across Vietnam. Standardizing and unifying AW3D30 DEM data according to the national height system will enhance the accuracy of topographic data, paving the way for new approaches in utilizing and applying geospatial data in Vietnam.

## 2. Materials and Methods

### 2.1. Methods

#### 2.1.1. Adjusting global elevation to local elevation

The AW3D30 global digital elevation model provides elevation referenced to the global geoid based on EGM96, within the tide-free system. In contrast, Vietnam's national vertical datum uses the multi-year mean sea level at Hon Dau Island, Hai Phong, within the mean-tide system. To adjust the elevation of the AW3D30 global digital elevation model to the national vertical datum, GNSS/levelling survey data (height control points) are utilized, specifically as follows:

Adjust the height anomaly of GNSS/levelling points derived from the global gravity field model EGM96 in the tide-free system to the mean-tide system using equation 1 [31, 54]:

$$\zeta_i^{\text{mean}} = \zeta_i^{\text{free}} + (1+k)(0,099 - 0,29 \sin^2 B_i) \quad (1)$$

In this study, the Earth is considered a rigid body, then  $k = 0$ .

The difference in height anomalies of GNSS/levelling points in the mean-tide system, as determined from the global gravity field model EGM96 and measured data, is calculated using equation 2:

$$\Delta\zeta_i = \zeta^{\text{GNSS/levelling}} - \zeta_i^{\text{mean}} \quad (2)$$

The elevations of GNSS/levelling points, extracted from the AW3D30 global digital elevation model and converted to the national vertical datum, are calculated using Equation 3:

$$H_i^{\text{reg}} = H_i^{\text{AW3D30}} + \Delta\zeta_i \quad (3)$$

where  $\zeta^{\text{free}}$  is the global height anomaly extracted from the EGM96 model in the free-tide system;  $\zeta^{\text{mean}}$  is the global height anomaly in the mean-tide system;  $\zeta^{\text{GNSS/levelling}}$  is the height anomaly measured at GNSS/levelling points;  $\Delta\zeta$  is the difference between the global height anomaly extracted from the EGM96 model and the measured height anomaly at GNSS/levelling points;  $H^{\text{AW3D30}}$  is the global elevation extracted from the AW3D30 model;

$H_i^{reg}$  is the global elevation in the national vertical datum after tidal correction;  $i$  is the index of the GNSS/levelling point.

### 2.1.2. Verification of AW3D30 global elevation data after conversion to the national vertical datum

#### a) Check for raw bias

The difference between the elevation of the AW3D30 global digital elevation model, after being adjusted to the national vertical datum, and the actual surveyed elevation at GNSS/levelling points is determined using equation 4:

$$\Delta_i = H_i^{reg} - H_i^{GNSS/levelling} \quad (4)$$

where  $\Delta$  is the difference between the elevation of the AW3D30 global digital elevation model, after being converted to the national vertical datum, and the measured elevation at GNSS/levelling points.

The mean value of the deviation between the elevation of the AW3D30 global digital elevation model, after being converted to the national vertical datum, and the measured elevation at GNSS/levelling points is determined according to equation 5:

$$\Delta_{aver} = \frac{\sum_i^n \Delta_i}{n} \quad (5)$$

where  $\Delta_{aver}$  is the mean height deviation of  $n$  points.

The deviation value between  $\Delta$  and  $\Delta_{aver}$  is calculated using equation 6:

$$d_i = \Delta_i - \Delta_{aver} \quad (6)$$

The standard deviation of the height error of the AW3D30 global digital elevation model in the national vertical datum, compared to the measured height at GNSS/levelling points, is calculated using equation 7:

$$\sigma = \sqrt{\frac{[dd]}{n-1}} \quad (7)$$

where  $\sigma$  is the standard deviation of the elevation from the AW3D30 global digital elevation model after being converted to the national vertical datum.

The standard deviation is used to assess the stability of the elevation data from the AW3D30 global digital elevation model in the national vertical datum. The threshold error limit ( $\Delta_{limit}$ ) is chosen to represent the distribution of data around the mean value as  $3\sigma$ , this means that  $\Delta_{limit} = \pm 3\sigma$ , corresponding to approximately 99.7% of the data falling within this range [55].

#### b) Check for systematic bias

The deviation between the elevation from the AW3D30 global digital elevation model, after being adjusted to the national vertical datum, and the actual surveyed elevation at GNSS/levelling points must satisfy inequality 8:

$$|[\Delta]| \leq 0,25[|\Delta|] \quad (8)$$

If inequality (8) is not satisfied, it indicates the presence of a systematic bias in the series of height deviations between the AW3D30 global digital elevation model in the national vertical datum and the measured heights. Therefore, correction is required.

The correction value is determined based on the deviation between the elevation from the AW3D30 global digital elevation model in the national vertical datum and the actual surveyed elevation at GNSS/levelling points, calculated using equation 9:

$$\theta = \frac{[\Delta]}{k} \quad (9)$$



where  $\theta$  is the correction value, and  $k$  is the total number of GNSS/levelling points used in the calculation.

The elevation value from the AW3D30 global digital elevation model, after being converted to the national vertical datum, is further corrected according to equation 10:

$$H_i^{local} = H_i^{reg} + \theta \tag{10}$$

where  $H_i^{local}$  is the elevation from the AW3D30 global digital elevation model after being converted to the national vertical datum and adjusted to eliminate systematic bias.

The deviation value between the elevation from the AW3D30 global digital elevation model, after verification, and the actual surveyed elevation at GNSS/levelling points in the national vertical datum is calculated using equation 11:

$$\varepsilon_i = H_i^{local} - H_i^{GSNN/levelling} \tag{11}$$

where  $\varepsilon$  represents the deviation between the elevation from the AW3D30 global digital elevation model, after adjustment, and the actual surveyed elevation at GNSS/levelling points in the national vertical datum.

The accuracy of the elevation from the AW3D30 global digital elevation model in the national vertical datum is assessed through the root mean square error (RMSE), calculated using equation 12:

$$m = \sqrt{\frac{[\varepsilon\varepsilon]}{2k}} \tag{12}$$

The standardization of the elevation of the global digital elevation model AW3D30 to Vietnam's national height system is summarized in the following diagram:

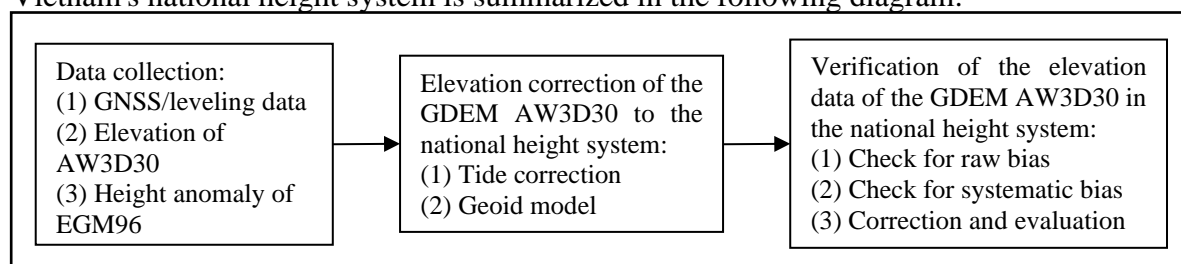


**Figure 1.** The standardization process of the AW3D30 GDEM in the national height system.

## 2.2. Data

The study area of this paper includes Ninh Binh province and adjacent regions in northern Vietnam. This area exhibits diverse topography, transitioning from low-lying plains to low hills. The average elevation ranges from 10 to 150 meters above sea level. Most of the region belongs to the Red River Delta, with elevations between 5 and 20 meters, while areas with elevations exceeding 100 meters are primarily concentrated in the west, along the edges of low mountain ranges.

For this study, 36 national GNSS/levelling of class I, II, and III (managed by the Department of Survey, Mapping, and Geographic Information Vietnam) within the region were used as reference points to transform the elevation of the AW3D30 global digital elevation model into the national vertical datum of Vietnam [31]. These points were also employed to assess the model's accuracy after correction (Figure 2).

Detailed information on the GNSS/levelling points is presented in Table 1. The parameters include geographic coordinates ( $B$ ,  $L$ ), elevation in the national vertical datum ( $h$ ), geoid undulation ( $\zeta$ ), elevation from the AW3D30 global digital elevation model ( $H^{AW3D30}$ ), which was obtained from JAXA's website, and geoid undulation from the EGM96 model ( $\zeta^{EGM96}$ ), retrieved from NGA's website. The specific values are listed in Table 1.

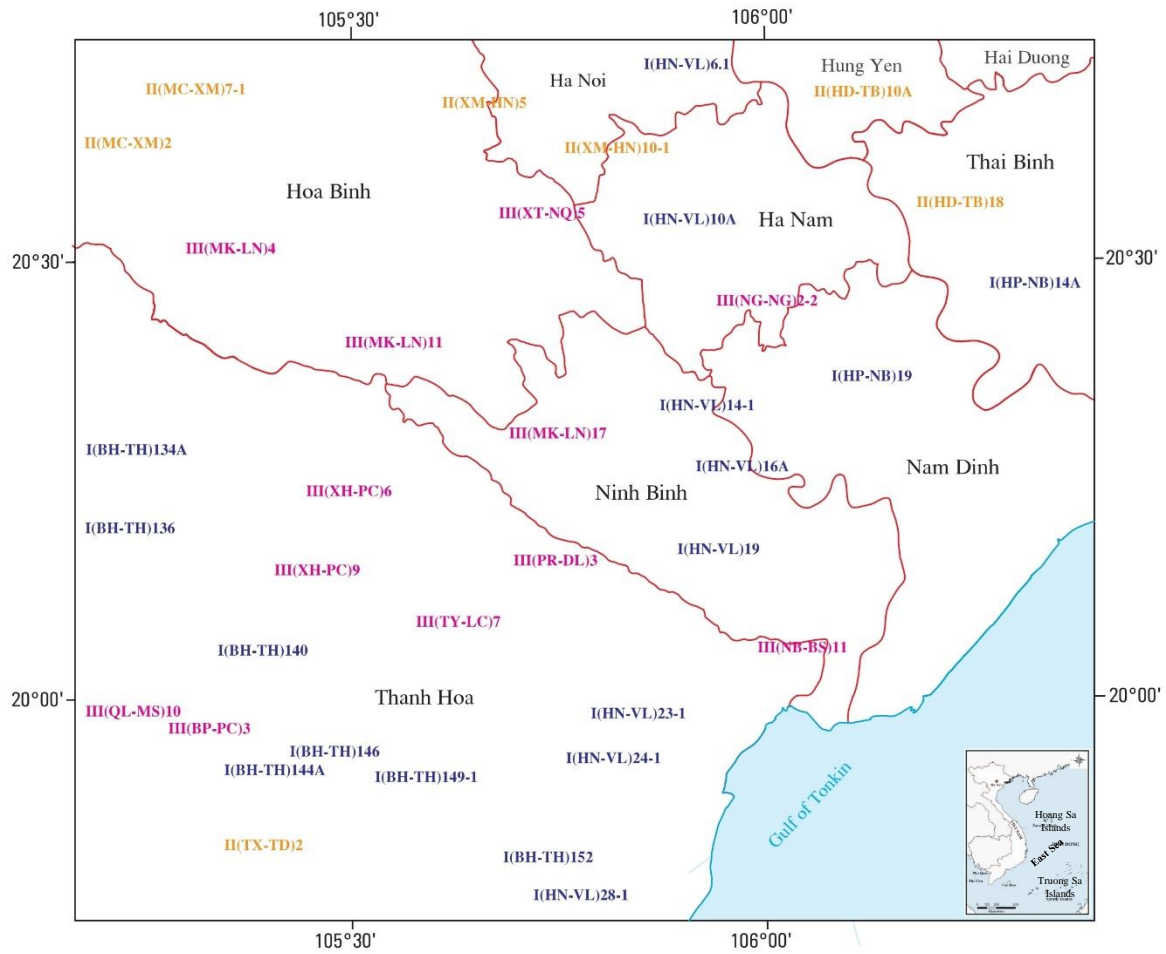


Figure 2. The experimental area includes Ninh Binh province and its surrounding areas.

Table 1. Data of GNSS/Levelling.

| N <sup>o</sup> | Point name    | B (°)    | L (°)     | h (m)   | ζ (m)    | H <sup>AW3D30</sup> (m) | ζ <sup>EGM96</sup> (m) |
|----------------|---------------|----------|-----------|---------|----------|-------------------------|------------------------|
| 1              | I(BH-TH)140   | 20.05652 | 105.39390 | 33.286  | -25.576  | 38.491                  | -26.836                |
| 2              | I(BH-TH)144A  | 19.91975 | 105.40804 | 17.292  | -25.495  | 22.241                  | -26.531                |
| 3              | I(BH-TH)146   | 19.94081 | 105.48019 | 13.075  | -25.275  | 17.445                  | -26.383                |
| 4              | I(HN-VL)10A   | 20.54737 | 105.91174 | 4.701   | -25.726  | 7.388                   | -25.917                |
| 5              | I(HN-VL)14-1  | 20.33468 | 105.93127 | 1.579   | -25.240  | 3.371                   | -25.445                |
| 6              | I(HN-VL)16A   | 20.26464 | 105.97354 | 1.621   | -25.112  | 7.829                   | -25.130                |
| 7              | I(HN-VL)19    | 20.17042 | 105.94407 | 1.017   | -24.897  | 4.004                   | -25.116                |
| 8              | I(HN-VL)23-1  | 19.98303 | 105.84626 | 6.273   | -24.633  | 9.387                   | -25.191                |
| 9              | I(HN-VL)24-1  | 19.93214 | 105.81605 | 3.262   | -24.598  | 5.186                   | -25.211                |
| 10             | I(HN-VL)6-1   | 20.72451 | 105.90901 | 3.004   | -26.0805 | 5.878                   | -26.341                |
| 11             | I(HP-NB)14A   | 20.47301 | 106.35673 | 0.805   | -25.0529 | 1.234                   | -23.886                |
| 12             | I(HP-NB)19    | 20.36705 | 106.13044 | 2.820   | -24.9932 | 7.986                   | -24.548                |
| 13             | II(HD-TB)10A  | 20.70225 | 106.12370 | 2.633   | -25.7538 | 4.374                   | -25.283                |
| 14             | II(HD-TB)18   | 20.56484 | 106.23877 | 1.127   | -25.4052 | 2.815                   | -24.418                |
| 15             | II(MC-XM)7-1  | 20.69792 | 105.31415 | 191.545 | -26.7516 | 198.777                 | -27.879                |
| 16             | II(XM-HN)10-1 | 20.63084 | 105.81869 | 4.251   | -25.939  | 7.861                   | -26.518                |
| 17             | II(XM-HN)5    | 20.68137 | 105.66371 | 9.087   | -26.220  | 13.732                  | -27.176                |
| 18             | III(BP-PC)3   | 19.96750 | 105.32913 | 49.300  | -25.667  | 52.902                  | -26.803                |
| 19             | III(MK-LN)11  | 20.40808 | 105.55323 | 35.336  | -25.799  | 41.181                  | -27.117                |
| 20             | III(MK-LN)17  | 20.30344 | 105.75076 | 2.521   | -25.463  | 8.446                   | -26.234                |

| N <sup>0</sup> | Point name    | B (°)    | L (°)     | h (m)   | ζ (m)   | H <sup>AW3D30</sup> (m) | ζ <sup>EGM96</sup> (m) |
|----------------|---------------|----------|-----------|---------|---------|-------------------------|------------------------|
| 21             | III(MK-LN)4   | 20.51584 | 105.35620 | 58.724  | -26.364 | 63.531                  | -27.661                |
| 22             | III(NB-BS)11  | 20.05737 | 106.04462 | 1.175   | -24.471 | 4.972                   | -24.511                |
| 23             | III(NG-NG)2-2 | 20.45389 | 106.00441 | 1.553   | -25.389 | 3.686                   | -25.275                |
| 24             | III(PR-DL)3   | 20.16046 | 105.75938 | 86.750  | -25.012 | 88.596                  | -25.916                |
| 25             | III(TY-LC)7   | 20.08866 | 105.62975 | 10.772  | -24.995 | 16.318                  | -26.252                |
| 26             | III(XH-PC)6   | 20.23835 | 105.49836 | 27.506  | -25.544 | 32.447                  | -26.967                |
| 27             | III(XH-PC)9   | 20.14820 | 105.43782 | 77.032  | -25.535 | 83.006                  | -26.929                |
| 28             | II(MC-XM)2    | 20.63549 | 105.18108 | 259.537 | -26.767 | 266.563                 | -28.018                |
| 29             | III(QL-MS)10  | 19.97696 | 105.21077 | 100.006 | -25.701 | 104.443                 | -27.064                |
| 30             | I(BH-TH)152   | 19.81928 | 105.73691 | 10.247  | -24.694 | 10.472                  | -25.300                |
| 31             | I(HN-VL)28-1  | 19.77585 | 105.77616 | 2.225   | -24.624 | 4.363                   | -25.073                |
| 32             | I(BH-TH)136   | 20.19649 | 105.22886 | 94.821  | -26.030 | 101.591                 | -27.420                |
| 33             | II(TX-TD)2    | 19.83409 | 105.39434 | 55.899  | -25.458 | 63.920                  | -26.419                |
| 34             | I(BH-TH)134A  | 20.28721 | 105.19301 | 59.512  | -26.190 | 67.154                  | -27.626                |
| 35             | I(BH-TH)149-1 | 19.91137 | 105.59042 | 8.669   | -24.883 | 16.540                  | -25.995                |
| 36             | III(XT-NQ)5   | 20.55524 | 105.73283 | 11.681  | -25.915 | 15.868                  | -26.736                |

### 3. Results and discussions

#### 3.1. Results

The analysis results of the national height control points in the study area (Table 1) were used to compute the global height anomaly in the mean tide system and to adjust the global elevation to the local height. These results are presented in Table 2.

**Table 2.** Adjustment of global elevation to local height.

| N <sup>0</sup> | Point name    | ζ <sup>mean</sup> (m) | H <sup>reg</sup> (m) | N <sup>0</sup> | Point name    | ζ <sup>mean</sup> (m) | H <sup>reg</sup> (m) |
|----------------|---------------|-----------------------|----------------------|----------------|---------------|-----------------------|----------------------|
| 1              | I(BH-TH)140   | -26.772               | 39.687               | 19             | III(MK-LN)11  | -27.054               | 42.435               |
| 2              | I(BH-TH)144A  | -26.466               | 23.212               | 20             | III(MK-LN)17  | -26.170               | 9.153                |
| 3              | I(BH-TH)146   | -26.319               | 18.489               | 21             | III(MK-LN)4   | -27.598               | 64.765               |
| 4              | I(HN-VL)10A   | -25.854               | 7.516                | 22             | III(NB-BS)11  | -24.447               | 4.947                |
| 5              | I(HN-VL)14-1  | -25.382               | 3.512                | 23             | III(NG-NG)2-2 | -25.212               | 3.510                |
| 6              | I(HN-VL)16A   | -25.066               | 7.783                | 24             | III(PR-DL)3   | -25.852               | 89.437               |
| 7              | I(HN-VL)19    | -25.053               | 4.159                | 25             | III(TY-LC)7   | -26.187               | 17.510               |
| 8              | I(HN-VL)23-1  | -25.126               | 9.881                | 26             | III(XH-PC)6   | -26.903               | 33.806               |
| 9              | I(HN-VL)24-1  | -25.147               | 5.735                | 27             | III(XH-PC)9   | -26.865               | 84.337               |
| 10             | I(HN-VL)6-1   | -26.279               | 6.077                | 28             | II(MC-XM)2    | -27.956               | 267.052              |
| 11             | I(HP-NB)14A   | -23.823               | 0.004                | 29             | III(QL-MS)10  | -26.999               | 105.741              |
| 12             | I(HP-NB)19    | -24.485               | 7.478                | 30             | I(BH-TH)152   | -25.235               | 11.013               |
| 13             | II(HD-TB)10A  | -25.221               | 3.842                | 31             | I(HN-VL)28-1  | -25.008               | 4.747                |
| 14             | II(HD-TB)18   | -24.355               | 1.765                | 32             | I(BH-TH)136   | -27.357               | 102.518              |
| 15             | II(MC-XM)7-1  | -27.817               | 199.242              | 33             | II(TX-TD)2    | -26.354               | 64.816               |
| 16             | II(XM-HN)10-1 | -26.456               | 8.378                | 34             | I(BH-TH)134A  | -27.562               | 68.526               |
| 17             | II(XM-HN)5    | -27.114               | 14.626               | 35             | I(BH-TH)149-1 | -25.930               | 17.587               |
| 18             | III(BP-PC)3   | -26.739               | 53.974               | 36             | III(XT-NQ)5   | -26.674               | 16.626               |

The deviation between the global elevation after conversion to local height and the elevation of the GNSS/levelling points is presented in Table 3 and Figure 3.



**Table 3.** Check the global elevation data AW3D30 after conversion to the national height.

| N <sup>o</sup> | Point name    | Δ (m)  | d (m)  | N <sup>o</sup> | Point name    | Δ (m) | d (m)  |
|----------------|---------------|--------|--------|----------------|---------------|-------|--------|
| 1              | I(BH-TH)140   | 6.402  | 1.589  | 19             | III(MK-LN)11  | 7.100 | 2.287  |
| 2              | I(BH-TH)144A  | 5.920  | 1.108  | 20             | III(MK-LN)17  | 6.633 | 1.820  |
| 3              | I(BH-TH)146   | 5.414  | 0.601  | 21             | III(MK-LN)4   | 6.041 | 1.229  |
| 4              | I(HN-VL)10A   | 2.815  | -1.997 | 22             | III(NB-BS)11  | 3.772 | -1.040 |
| 5              | I(HN-VL)14-1  | 1.933  | -2.880 | 23             | III(NG-NG)2-2 | 1.957 | -2.855 |
| 6              | I(HN-VL)16A   | 6.163  | 1.350  | 24             | III(PR-DL)3   | 2.687 | -2.125 |
| 7              | I(HN-VL)19    | 3.143  | -1.670 | 25             | III(TY-LC)7   | 6.738 | 1.926  |
| 8              | I(HN-VL)23-1  | 3.608  | -1.205 | 26             | III(XH-PC)6   | 6.301 | 1.488  |
| 9              | I(HN-VL)24-1  | 2.473  | -2.340 | 27             | III(XH-PC)9   | 7.305 | 2.492  |
| 10             | I(HN-VL)6-1   | 3.073  | -1.739 | 28             | II(MC-XM)2    | 7.515 | 2.703  |
| 11             | I(HP-NB)14A   | -0.801 | -5.614 | 29             | III(QL-MS)10  | 5.735 | 0.923  |
| 12             | I(HP-NB)19    | 4.659  | -0.154 | 30             | I(BH-TH)152   | 0.766 | -4.046 |
| 13             | II(HD-TB)10A  | 1.209  | -3.604 | 31             | I(HN-VL)28-1  | 2.522 | -2.290 |
| 14             | II(HD-TB)18   | 0.638  | -4.174 | 32             | I(BH-TH)136   | 7.697 | 2.885  |
| 15             | II(MC-XM)7-1  | 7.697  | 2.885  | 33             | II(TX-TD)2    | 8.917 | 4.105  |
| 16             | II(XM-HN)10-1 | 4.127  | -0.686 | 34             | I(BH-TH)134A  | 9.014 | 4.202  |
| 17             | II(XM-HN)5    | 5.539  | 0.727  | 35             | I(BH-TH)149-1 | 8.917 | 4.105  |
| 18             | III(BP-PC)3   | 4.674  | -0.138 | 36             | III(XT-NQ)5   | 4.945 | 0.133  |

The average value of the height deviation between the global elevation AW3D30 in the national vertical datum and the surveyed elevation of the GNSS/levelling points is:

$$\Delta_{\text{aver}} = \frac{173.248}{36} \approx 4.812(\text{m})$$

The standard deviation of the global elevation AW3D30 in the national vertical datum is:

$$\delta = \sqrt{\frac{227.647}{35}} \approx \pm 2.550(\text{m})$$

Thus, the limiting error is determined as  $\Delta_{\text{limit}} = \pm 3\sigma = \pm 7.650(\text{m})$ .

In the study area, the points II(TX-TD)2, I(BH-TH)134A, and I(BH-TH)149-1 have deviations between the global elevation AW3D30 in the national vertical datum and the actual surveyed elevation that exceed the allowable error limits, falling outside the range  $[-7.650, +7.650]$ , and were therefore excluded. As a result, 33 points remain, with deviations within the allowable error limits, accounting for approximately 91.7% of the total number of points. This shows that most of the study points have deviations within the permissible range, indicating that the AW3D30 global elevation model is highly compatible with the national vertical datum in the study area. Next, the systematic deviation is checked within the range of elevation values of the AW3D30 global elevation model in the national vertical datum.

From the data in Table 3, we calculate  $|\Delta| = 146.400(\text{m})$ ,  $0.25|\Delta| = 36.600(\text{m})$ . Therefore, inequality (8) is not satisfied, indicating the existence of a systematic deviation in the range of AW3D30 global elevation values compared to the national vertical datum. This systematic deviation is determined according to formula (9) as follows:

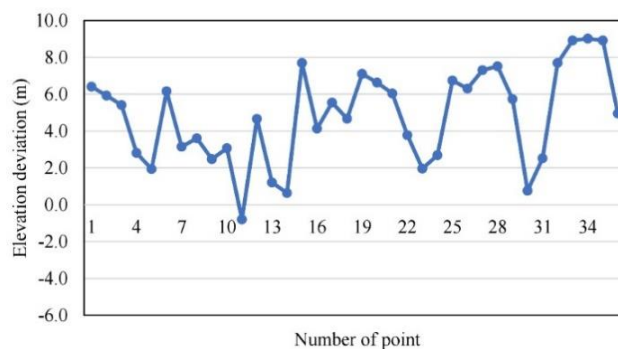


**Figure 3.** The deviation between the AW3D30 elevation in the national vertical datum and the elevation of the GNSS/levelling points.

$$\theta = \frac{[\Delta]}{m} = \frac{146.400}{33} \approx 4.436(m)$$

After the adjustment, the deviation between the AW3D30 global elevation and the elevation of the GNSS/levelling is shown in Figure 4.

From Figures 3 and 4, a significant improvement in the elevation deviation of the global digital elevation model AW3D30 can be observed after applying the correction. Before correcting raw errors and systematic errors, the absolute deviation between the AW3D30 model elevation and GNSS/levelling elevation reached up to 9.014 m, indicating a substantial discrepancy between the model data and actual measurements. However, after applying the correction method, the maximum absolute deviation was significantly reduced to 5.238 m.

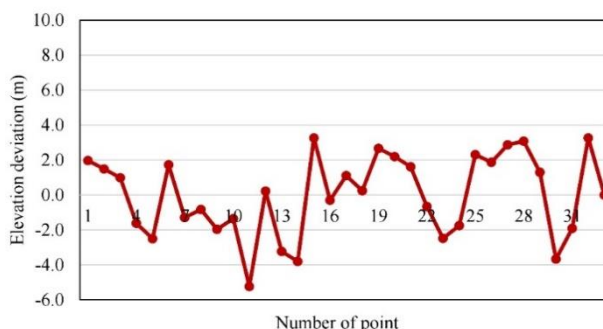


**Figure 4.** The deviation between the AW3D30 global elevation after adjustment and the elevation of the GNSS/levelling points.

Figure 4 shows that the elevation deviation values are randomly distributed around a mean value of zero, with no systematic trend. This indicates that systematic errors have been eliminated, and no residual errors remain after the correction. The root mean square error, representing the accuracy of the AW3D30 global digital elevation model in the national vertical reference system, is determined according to equation (12) and has a value of:  $m \approx \pm 1.613(m)$ .

The root mean square error of  $\pm 1.613$  m reflects the average accuracy of the AW3D30 global digital elevation model across the entire study area. This indicates that AW3D30 is capable of providing reliable elevation data after being adjusted to the national elevation system.

### 3.2. Discussions

The AW3D30 GDEM has been assessed for accuracy within the national height system in Ninh Bình and its surrounding areas, with a determined root mean square error (RMSE) of  $\pm 1.613$  m. This value reflects the average error level when compared to reference elevation data in the study area. Compared to previous studies summarized in Table 4, the RMSE of AW3D30 in Ninh Bình and its vicinity is significantly lower than in many other regions. This can be attributed to the topographical characteristics of Ninh Bình, which mainly consists of karst terrain with limestone hills interspersed with plains but without excessively steep slopes, along with an appropriate DEM correction method that helps reduce model errors. Therefore, AW3D30 can be considered a reliable DEM for applications in terrain studies, planning, and environmental management in this region.

**Table 4.** Accuracy of the AW3D30 GDEM in some areas.

| No | References | Regions/countries                                  | Accuracy (m) | Topographic characteristics   |
|----|------------|--|--------------|---|
| 1  | [20]       | Near Istanbul, Turkey                              | 2.49         | Terrain with a slope < 10%  |
| 2  | [21]       | Nigeria, West Africa                               | 5.67         | Predominantly flat or slightly sloping terrain, with an average elevation < 200 m |
| 3  | [23]       | Peru   | 2.172        | Tropical forest terrain with many rivers and wide basins                          |
| 4  | [51]       | Southwest Australia and northern Bangkok, Thailand | 4.4          | Mountainous and lowland terrain   |

| No | References | Regions/countries  | Accuracy (m)                    | Topographic characteristics       |
|----|------------|--|---------------------------------|-----------------------------------|
| 5  | [52]       | Eurasia, North America, South America, Australia, Africa | 2.49                            | Lowland terrain                   |
|    |            |  | 2.64                            | Terrain with a slope of 10° - 20° |
| 6  | [53]       | North America, Europe, Asia, Africa, South America       | 2-4                             | Flat terrain                      |
|    |            | This study   | Ninh Binh and surrounding areas | 1.613                             |

#### 4. Conclusion

This study has converted the global elevation of the AW3D30 global digital elevation model to the national vertical datum of Vietnam through a calibration process. The experiment was conducted in Ninh Bình Province and surrounding areas. The calibration method consists of three main steps: (1) converting the elevation of the AW3D30 model from the global vertical datum to the national vertical datum based on GNSS/levellings; (2) removing points with significant discrepancies exceeding the permissible threshold to ensure the model's stability; (3) performing system error correction to minimize the overall discrepancy between the AW3D30 model data and the GNSS/levelling data.

The experimental results show that after applying the correction method, the root mean square error of the AW3D30 model in the national vertical datum is  $\pm 1.613$  m. At the same time, the maximum discrepancy between the height of the AW3D30 model and the height of GNSS/levelling points decreased from 9.014 m to 5.238 m. Statistical analysis also shows that 91.7% of the control points have discrepancies within the allowable limits, indicating that the correction method has significantly improved the accuracy and compatibility of the AW3D30 model with Vietnam's national vertical datum in the study area.

With an accuracy of  $\pm 1.613$  m in the study area, the global digital elevation model AW3D30 demonstrates high reliability in representing terrain. Standardizing the elevation of this model within the national vertical datum not only ensures consistency with domestic survey data but also facilitates practical applications. As a result, AW3D30 can be effectively utilized in various fields such as topographic mapping, urban planning, natural resource management, and terrain change monitoring.

In this study, the conversion of elevations from the global digital elevation model to the national vertical datum was conducted rigorously. The results obtained in the study area indicate that this method not only harmonizes elevation data with the national reference system but also enhances the model's accuracy. With its flexibility and broad applicability, this method can be effectively implemented in other regions, particularly in topographic studies and territorial spatial management.

This research focuses on lowland and low-hill areas, using data from the nation's first-order, second-order, and third-order GNSS/levelling points-high-precision control points as the basis for converting and assessing the accuracy of the AW3D30 global digital elevation model within the national vertical datum. To gain a more comprehensive understanding of AW3D30's performance across Vietnam, further studies should extend to regions with more complex and diverse terrain, such as high mountainous areas, transitional zones between plains and hills, or coastal regions. Additionally, experimenting with other correction methods during evaluation would provide more detailed insights into the model's errors under different terrain conditions. This would help determine the suitability and practical applicability of AW3D30, particularly in surveying, planning, and resource management.

**Author contribution statement:** The development of the idea, design, data collection, experimental calculations, and draft writing: B.T.H.T.; Draft revision and calculation result verification: T.T.H.T.; Draft revision and calculation result verification: D.T.H.

**Acknowledgements:** This research is funded by the Ministry of Natural Resources and Environment through the Ministry-level scientific research project, project code: TNMT.2024.04.04. We would like to express our sincere gratitude to the Ministry of Natural Resources and Environment for providing the necessary resources and support during the course of this research.

**Competing interest statement:** The authors declare no conflict of interest.

## References

1. Yang, L.; Meng, X.; Zhang, X. SRTM DEM and its application advances. *Int. J. Remote Sens.* **2011**, *32*, 3875–3896.
2. Hirt, C.; Marti, U.; Bürki, B.; Featherstone, W.E. Assessment of EGM2008 in Europe using accurate astrogeodetic vertical deflections and omission error estimates from SRTM/DTM2006.0 residual terrain model data. *J. Geophys. Res.* **2010**, *115*, B10404.
3. Józsa, E.; Fábrián, S.A.; Kovács, M. An evaluation of EU–DEM in comparison with ASTER GDEM, SRTM and contour-based DEMs over the Eastern Mecsek Mountains. *Hung. Geogr. Bull.* **2014**, *63*, 401–423.
4. Akbari, A.; Abu, S.A.; Othman, F. Integration of SRTM and TRMM data into the GIS–based hydrological model for the purpose of flood modelling. *Hydrol. Earth Syst. Sci. Discuss.* **2012**, *9*, 4747–4775.
5. Domeneghetti, A. On the use of SRTM and altimetry data for flood modeling in data–sparse regions. *Water Resour. Res.* **2016**, *52*, 2901–2918.
6. Hancock, G.R.; Martinez, C.; Evans, K.G.; Moliere, D.R. A comparison of SRTM and high–resolution digital elevation models and their use in catchment geomorphology and hydrology: Australian examples. *Earth Surf. Processes Landforms* **2006**, *31*, 1394–1412.
7. Taramelli, A.; Melelli, L. Map of deep seated gravitational slope deformations susceptibility in central Italy derived from SRTM DEM and spectral mixing analysis of the Landsat ETM + data. *Int. J. Remote Sens.* **2009**, *30*, 357–387.
8. Triarahmadhana, B.; Heliani, L.S. An evaluation of the use of SRTM data to the accuracy of local geoid determination: A case study of Yogyakarta Region, Indonesia. Proceeding of the 12<sup>th</sup> Biennial Conference of Pan Ocean Remote Sensing Conference (PORSEC 2014). 2014.
9. Blitzkow, D.; de Matos, A.C.; Cintra, J.P. Digital terrain model evaluation and computation of the terrain correction and indirect effect in South America. *Asociación Argentina de Geofísicos y Geodestas* **2009**, *34*, 59–74.
10. Monteiro, E.S.; Fonte, C.C.; de Lima, J.L. Improving the positional accuracy of drainage networks extracted from global digital elevation models using OpenStreetMap data. *J. Hydrol. Hydromech.* **2018**, *66*, 285–294.
11. Ibrahim, M.; Al-Mashaqbah, A.; Koch, B.; Datta, P. An evaluation of available digital elevation models (DEMs) for geomorphological feature analysis. *Environ. Earth Sci.* **2020**, *79*, 336.
12. Oliveira, P.T.S.; Rodrigues, D.B.B.; Sobrinho, T.A.; Panachuki, E.; Wendland, E. Use of SRTM data to calculate the (R)USLE topographic factor. *Acta Scientiarum Technol.* **2013**, *35*, 507–513.
13. Xu, K.; Fang, J.; Fang, Y.; Sun, Q.; Wu, C.; Liu, M. The importance of digital elevation model selection in flood simulation and a proposed method to reduce DEM errors: a case study in Shanghai. *Int. J. Disaster Risk Sci.* **2021**, *12*, 890–902.
14. Khattab, M.I.; Abotalib, A.Z.; Othman, A.; Selim, M.K. Evaluation of multiple digital elevation models for hypsometric analysis in the watersheds affected by the opening of the Red Sea the Egyptian. *J. Remote Sens. Space Sci.* **2023**, *26*, 1020–1035.
15. Okolie, C.J.; Mills, J.P.; Adeleke, A.K.; Smit, J.L.; Peppia, M.V.; Altunel, A.O.; Arungwa, I.D. Assessment of the global Copernicus, NASADEM, ASTER and AW3D digital elevation models in Central and Southern Africa. *Geo-Spatial Inf. Sci.* **2024**, *27*, 1362–1390.
16. Uuemaa, E.; Ahi, S.; Montibeller, B.; Muru, M.; Kmoch, A. Vertical accuracy of freely

- available global digital elevation models (ASTER, AW3D30, MERIT, TanDEM-X, SRTM, and NASADEM). *Remote Sens.* **2020**, *12*, 3482.
17. Rodriguez, E.; Morris, C.S.; Belz, J.E.; Chapin, E.C.; Martin, J.M.; Daffer, W.; et al. An assessment of the SRTM topographic products, Technical Report JPL D-31639. Pasadena, California: Jet Propulsion Laboratory. 2005.
  18. Bettioli, G.M.; Ferreira, M.E.; Motta, L.P.; Cremon, É.H.; Sano, E.E. Conformity of the NASADEM\_HGT and ALOS AW3D30 dem with the altitude from the Brazilian geodetic reference stations: A case study from Brazilian Cerrado. *Sensors* **2021**, *21*, 2935.
  19. Chen, X.; Zhang, Q.; Cheng, C.; Zhou, X.; Yu, X. Accuracy assessment of SRTM DEM, ASTER GDEM, AW3D30 DSM, and TanDEM-X 90 m DEM based on runway elevation data. Proceeding of the 2022 2<sup>nd</sup> International Conference on Big Data, Artificial Intelligence and Risk Management (ICBAR). IEEE. 2022.
  20. Bayburt, S.; Kurtak, A.; Büyüksalih, G.; Jacobsen, K. Geometric accuracy analysis of WorldDEM in relation to AW3D30, SRTM and ASTER GDEM2. The International Archives of the Photogrammetry. *Remote Sens. Spatial Inf. Sci.* **2017**, *42*, 211–217.
  21. Apeh, O.; Uzodinma, V.; Ebinne, E.; Moka, E.; Onah, E. Accuracy assessment of ALOS W3d30, ASTER GDEM and SRTM30 DEM: A case study of Nigeria, West Africa. *J. Geogr. Inf. Syst.* **2019**, *11*, 111.
  22. Güvenç, M. Comparative evaluation of vertical accuracy of ground control points from ASTER-DEM SRTM-DEM with respect to ALOS-DEM. Hasan Kalyoncu Üniversitesi. 2020.
  23. del Rosario, G.M.M.; Viveen, W.; Vidal-Villalobos, R.A.; Villegas-Lanza, J.C. A performance comparison of SRTM v. 3.0, AW3D30, ASTER GDEM3, Copernicus and TanDEM-X for tectonogeomorphic analysis in the south American Andes. *Catena* **2023**, *228*, 107160.
  24. Hnila, P.; Elicker, J. Quality assessment of digital elevation models in a Treeless high-mountainous landscape: A case study from Mount Aragats, Armenia. *Magazen* **2021**, *2*, 71–102.
  25. Zhao, S.; Cheng, W.; Zhou, C.; Chen, X.; Zhang, S.; Zhou, Z.; et al. Accuracy assessment of the ASTER GDEM and SRTM3 DEM: an example in the Loess Plateau and North China Plain of China. *Int. J. Remote Sens.* **2011**, *32*, 8081–8093.
  26. Yao, J.; Chao-lu, Y.; Ping, F. Evaluation of the accuracy of SRTM3 and ASTER GDEM in the Tibetan Plateau Mountain Ranges. *E3S Web Conf.* **2020**, *206*, 01027.
  27. Mukherjee, S.; Joshi, P.K.; Mukherjee, S.; Ghosh, A.; Garg, R.D.; Mukhopadhyay, A. Evaluation of vertical accuracy of open source Digital Elevation Model (DEM). *Int. J. Appl. Earth Obs. Geoinf.* **2013**, *21*, 205–217.
  28. Tachikawa, T.; Kaku, M.; Iwasaki, A.; Gesch, D.B.; Oimoen, M.J.; Zhang, Z.; et al. ASTER global digital elevation model version 2—summary of validation results. NASA. 2011.
  29. Hirt, C.; Filmer, M.S.; Featherstone, W.E. Comparison and validation of the recent freely available ASTER-GDEM ver1, SRTM ver4.1 and GEODATA DEM-9s Ver3 digital elevation models over Australia. *Aust. J. Earth Sci.* **2010**, *57*, 337–347.
  30. Farr, T.G.; Rosen, P.A.; Caro, E.; Crippen, R.; Duren, R.; Hensley, S.; et al. The shuttle radar topography mission. *Rev. Geophys.* **2007**, *45*, RG2004.
  31. Tham, B.T.H.; Thanh, T.P. Correction of global elevation data SRTM to the national elevation system in the territory of Vietnam. *Aust. J. Earth Sci.* **2025**, 1–10.
  32. Smith, B.; Sandwell, D. Accuracy and resolution of shuttle radar topography mission data. *Geophys. Res. Lett.* **2003**, *30*(9), 1467.
  33. Rodriguez, E.; Morris, C.S.; Belz, J.E. A global assessment of the SRTM performance. *Photogramm. Eng. Remote Sens.* **2006**, *72*, 249–260.
  34. Gesch, D.; Oimoen, M.; Greenlee, S.; Nelson, C.; Steuck, M.; Tyler, D. The national elevation dataset. *Photogramm. Eng. Remote Sens.* **2002**, *68*, 5–32.
  35. Höhle, J.; Höhle, M. Accuracy assessment of digital elevation models by means of robust



- statistical methods. *ISPRS J. Photogramm. Remote Sens.* **2009**, 64, 398–406.
36. Arun, P.V. A comparative analysis of different DEM interpolation methods. *Egypt. J. Remote Sens. Space. Sci.* **2013**, 16, 133–139.
  37. Liu, X. Accuracy assessment of LiDAR elevation data using survey marks. *Surv. Rev.* **2011**, 43, 80–93.
  38. Sithole, G.; Vosselman, G. Experimental comparison of filter algorithms for bare-Earth extraction from airborne laser scanning point clouds. *ISPRS J. Photogramm. Remote Sens.* **2004**, 59, 85–101.
  39. Zhang, K.; Whitman, D. Comparison of three algorithms for filtering airborne lidar data. *Photogramm. Eng. Remote Sens.* **2005**, 71, 313–324.
  40. Hengl, T.; Heuvelink, G.B.; Stein, A. A generic framework for spatial prediction of soil variables based on regression-kriging. *Geoderma* **2004**, 120, 75–93.
  41. Gopal, S. Artificial neural networks for spatial data analysis. NCGIA Core Curriculum in GIScience. 1998.
  42. Goovaerts, P. Geostatistics for natural resources evaluation. Oxford University Press. 1997.
  43. Lloyd, C.D.; Atkinson, P.M. Deriving ground surface digital elevation models from LiDAR data with geostatistics. *Int. J. Geogr. Inf. Sci.* **2006**, 20, 535–563.
  44. Webster, R.; Oliver, M.A. Geostatistics for environmental scientists. John Wiley & Sons. 2007.
  45. Hengl, T.; Heuvelink, G.B.; Rossiter, D.G. About regression-kriging: From equations to case studies. *Comput. Geosci.* **2007**, 33, 1301–1315.
  46. Oliver, M.A.; Webster, R. A tutorial guide to geostatistics: Computing and modelling variograms and kriging. *Catena* **2014**, 113, 56–69.
  47. Thanh, N.T.; Bac, N.X.; Huan, H.D.; Chuong, N.T.; Hoa, N.T.Q. Accuracy assesment of shuttle radar topography mission SRTM in whole area of Vietnam. Proceedings of the Fundamental Research in "Earth and Environmental Sciences". 2019, pp. 222–225.
  48. Hoa, H.M.; Thuy, D.X. Estimation of ability of using of global digital terrain model with high resolution 1" x 1" for calculation of terrain corrections in mountainous regions of Vietnam. *J. Geod. Cartogr.* **2017**, 33, 1–10.
  49. Tham, B.T.H. Assessment of the Accuracy of the global digital elevation model SRTM in Vietnam. GIS 2015 Conference. 2015, pp. 639–643.
  50. Thach, L.T.; Hoan, P.X. Assessment of the global digital model based on Vietnam digital elevation model. *J. Geod. Cartogr.* **2021**, 1–7.
  51. Tadono, T.; Nagai, H.; Ishida, H.; Oda, F.; Naito, S.; Minakawa, K.; et al. Generation of the 30 M-mesh global digital surface model by ALOS PRISM. *Int. Arch. Photogramm. Remote Sens. Spatial Inf. Sci.* **2016**, 41, 157–162.
  52. Takaku, J.; Tadono, T.; Tsutsui, K.; Ichikawa, M. Validation of "AW3D" global DSM generated from Alos Prism. *ISPRS Ann. Photogramm. Remote Sens. Spatial Inf. Sci.* **2016**, 3, 25–31.
  53. Yamazaki, D.; Ikeshima, D.; Tawatari, R.; Yamaguchi, T.; O'Loughlin, F.; Neal, J.C.; et al. A high-accuracy map of global terrain elevations. *Geophys. Res. Lett.* **2017**, 44, 5844–5853.
  54. Ekman, M. Impacts of geodynamic phenomena on systems for height and gravity. *Bull. Géodésique* **1989**, 63, 281–296.
  55. Ghilani, C.D.; Wolf, P.R. Adjustment computations: Spatial data analysis. John Wiley & Sons, Inc, Hoboken, New Jersey. 2006.